New pincer-type gold(III) complexes: Synthesis, characterization, DNA binding studies and cytotoxicity

Snežana Radisavljević,[a] Ioannis Bratsos,[b] Andreas Scheurer,[c] Jana Korzekwa,[c] Romana Masnikosa,[d] Aleksandar Tot,[e] Nevenka Gligorijević,[f] Siniša Radulović[f] and Ana Rilak Simović[a]*

[a]*University of Kragujevac, Faculty of Science, R. Domanovića 12, P. O. Box 60, 34000 Kragujevac, Serbia.*

[b]*I.N.N., Department of Physical Chemistry, NCSR "Demokritos", 15310 Ag. Paraskevi, Athens, Greece.*

[c]*Inorganic Chemistry, Department of Chemistry and Pharmacy, University of Erlangen-Nürnberg, Erlangen, Germany*

[d]*Department of Physical Chemistry, Vinča Institute of Nuclear Sciences, University of Belgrade, Mike Petrovića Alasa 12-14, 11000 Belgrade, Serbia*

[e]*University of Novi Sad, Faculty of Sciences, Department of Chemistry, Biochemistry and Environmental Protection, Trg Dositeja Obradovića 3, 21000 Novi Sad, Serbia.*

[f]*Institute for Oncology and Radiology of Serbia, Pasterova 14, 11000 Belgrade, Serbia.*

**Corresponding author:* Dr. Ana Rilak Simović
Department of Chemistry,
Faculty of Science,
University of Kragujevac,
Radoja Domanovića 12
Tel: +381(0)34300262
Fax: +381(0)34335040
e-mail: anarilak@kg.ac.rs

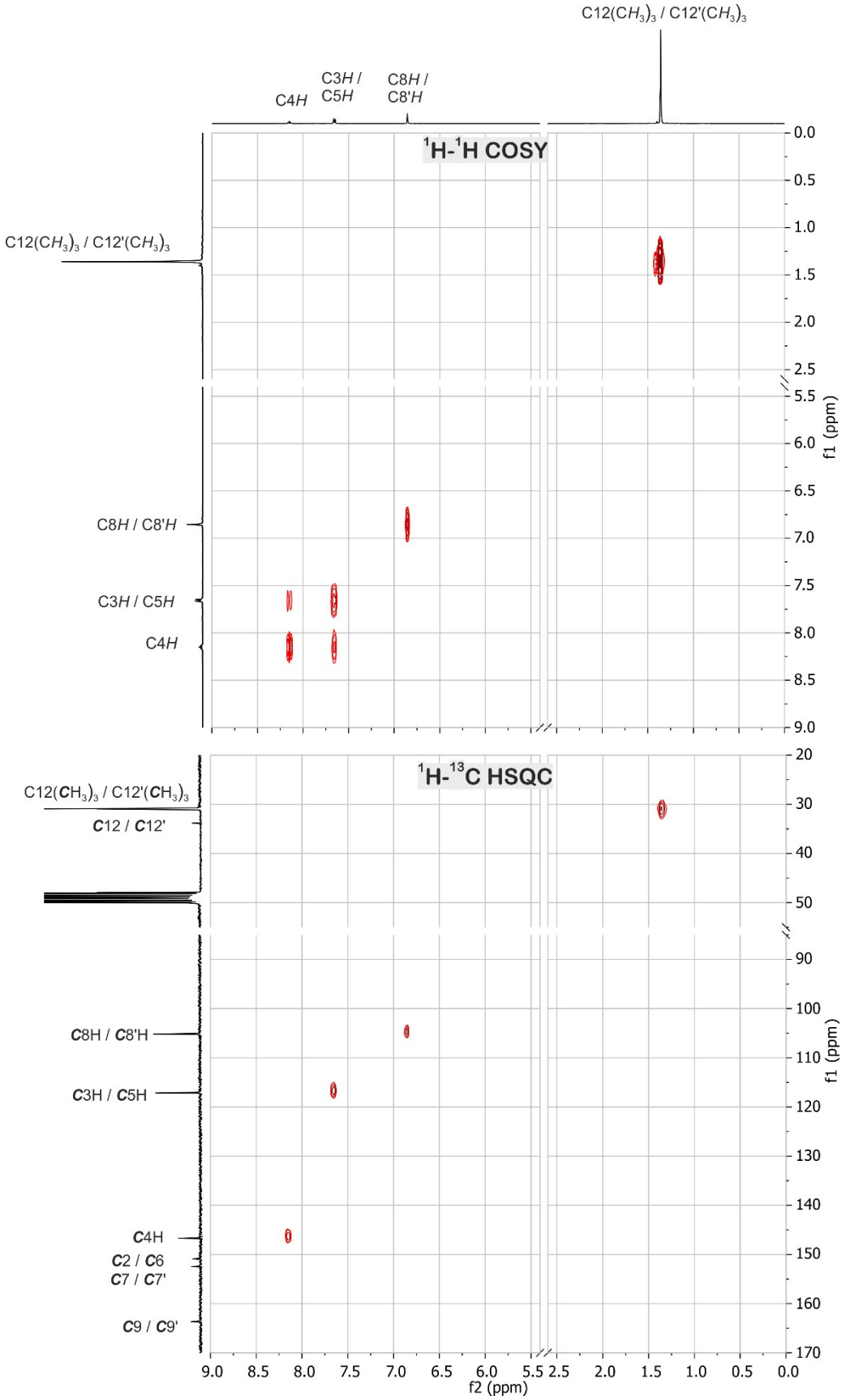

Fig. S1. The 2D homonuclear ^{1}H-^{1}H COSY (top) and heteronuclear ^{1}H-^{13}C HSQC (bottom) NMR spectra of complex **1** in CD_3OD at ambient temperature.

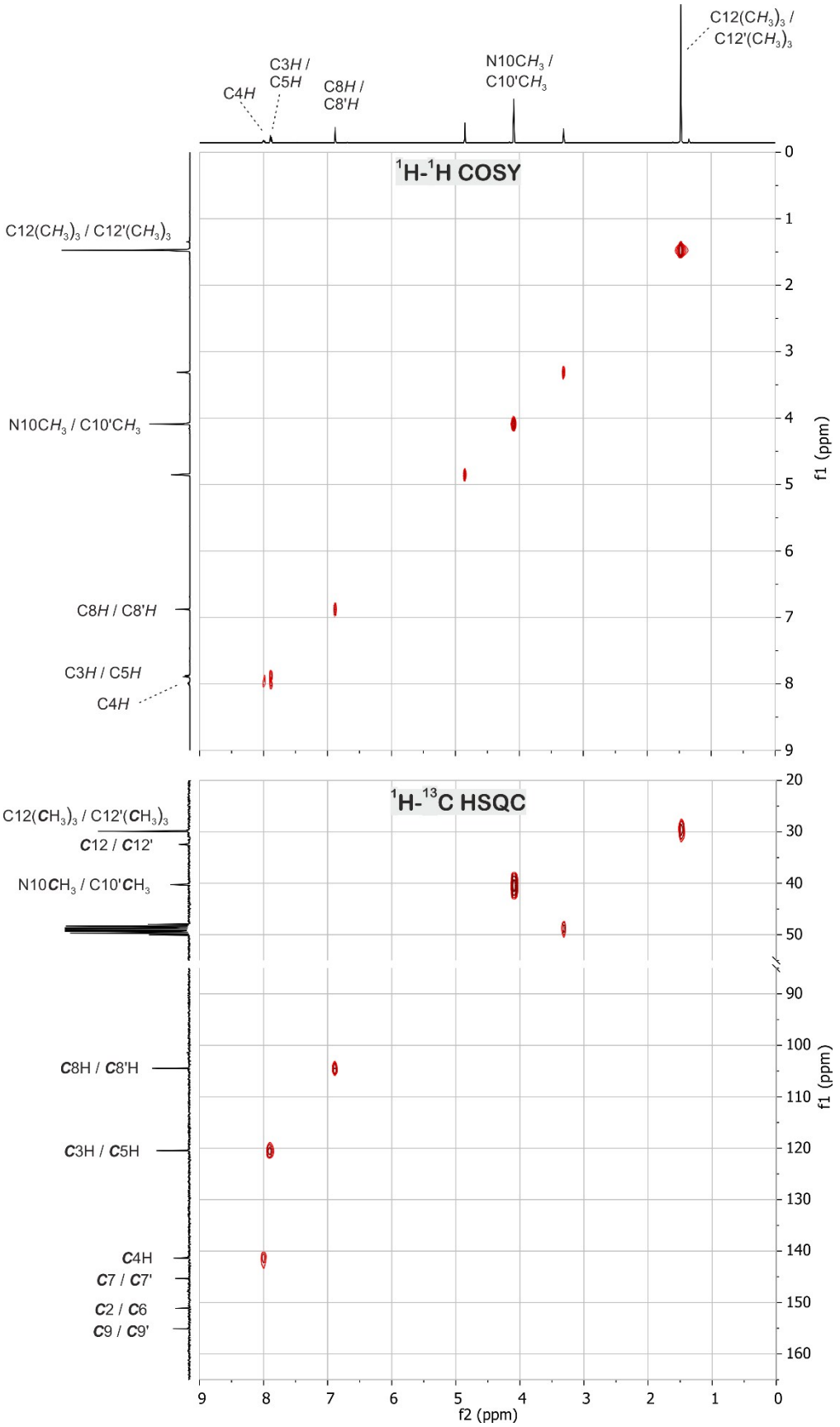

Fig. S2. The 2D homonuclear ^{1}H-^{1}H COSY (top) and heteronuclear ^{1}H-^{13}C HSQC (bottom) NMR spectra of complex **2** in CD_3OD at ambient temperature.

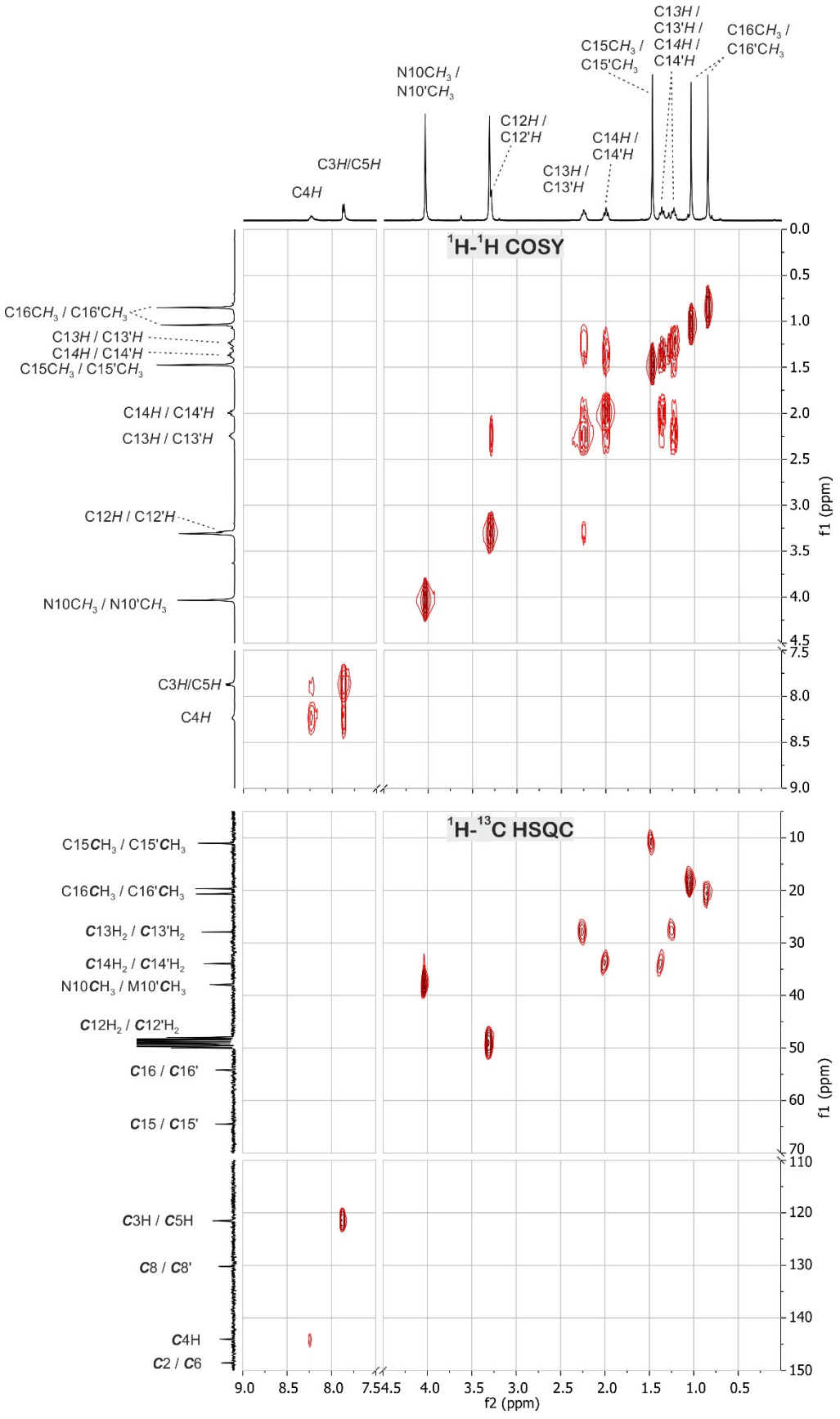
C4H
C3H/C5H
N10CH3 / N10'CH3
C12H / C12'H
C13H / C13'H
C14H / C14'H
C15CH3 / C15'CH3
C13H / C13'H / C14H / C14'H
C16CH3 / C16'CH3
1H-1H COSY
f1 (ppm)
1H-13C HSQC
C15CH3 / C15'CH3
C16CH3 / C16'CH3
C13H2 / C13'H2
C14H2 / C14'H2
N10CH3 / M10'CH3
C12H2 / C12'H2
C16 / C16'
C15 / C15'
C3H / C5H
C8 / C8'
C4H
C2 / C6
f2 (ppm)

Fig. S3. The 2D homonuclear ^{1}H-^{1}H COSY (top) and heteronuclear ^{1}H-^{13}C HSQC (bottom) NMR spectra of complex **3** in CD_3OD at ambient temperature.

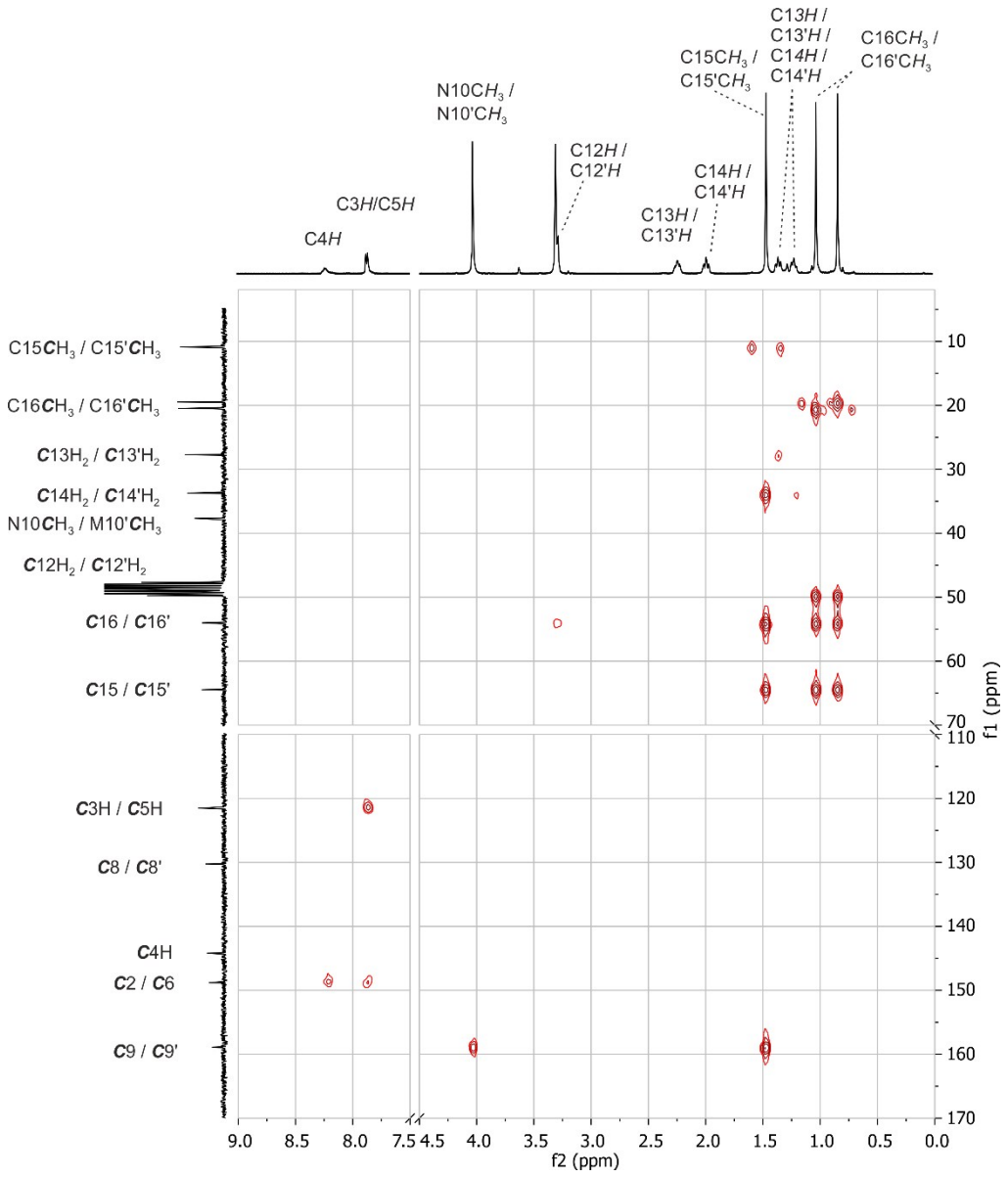

Fig. S4. The 2D heteronuclear ^{1}H-^{13}C HMQC NMR spectrum of complex **3** in CD_3OD at ambient temperature.

A

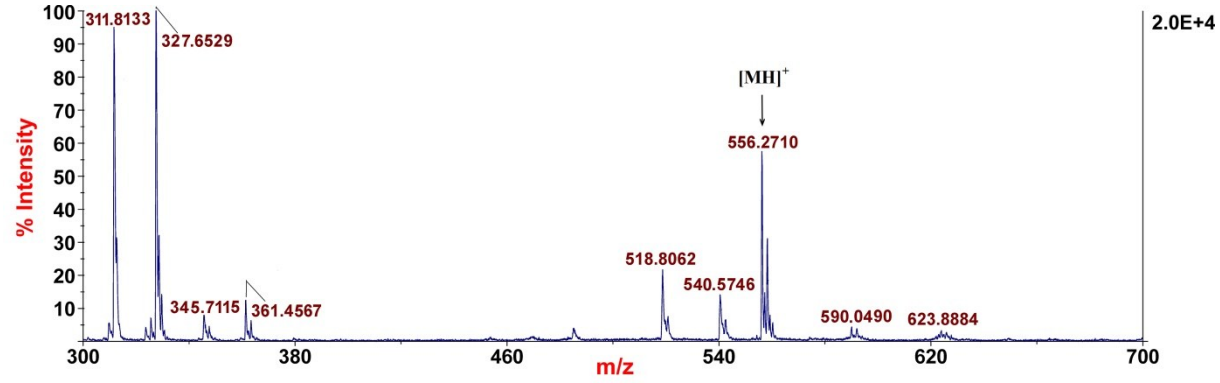

B

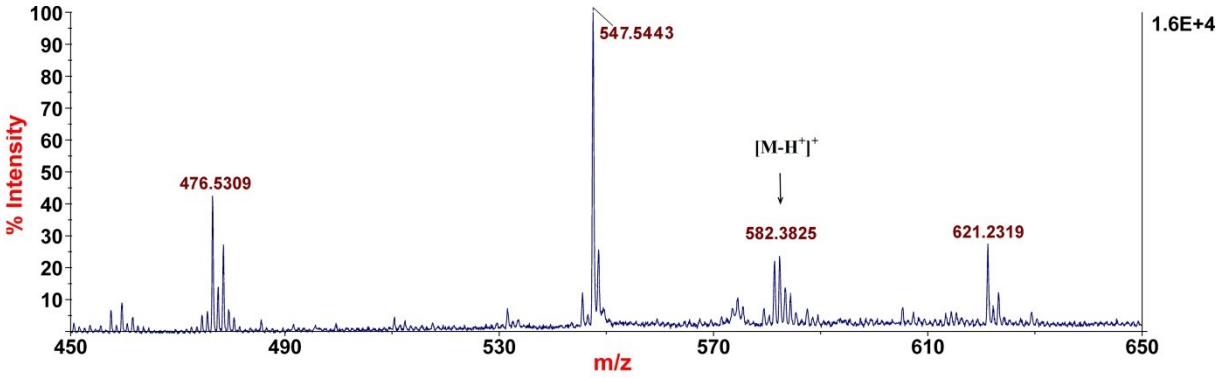

C

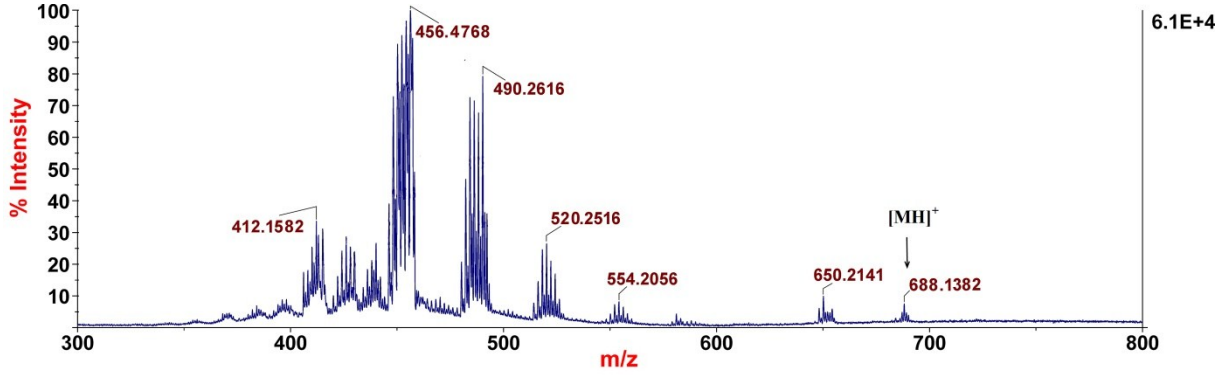

Fig. S5. MALDI TOF mass spectra of the complexes **1** (A), **2** (B) and **3** (C). The spectra were acquired in the positive reflectron mode, by averaging at least 300 laser shots. Instrumental settings were as follows: A) accelerating voltage 9000 V, grid voltage 40%, extraction delay time 180 ns, laser intensity 2825; B) accelerating voltage 12000 V, grid voltage 70%, extraction delay time 160 ns, laser intensity 3265; C) accelerating voltage 20000

V, grid voltage 80%, extraction delay time 100 ns, laser intensity 3100. In all cases, the guide wire was 0.05%, acquisition mass range 100 – 1000 *m/z* and the low mass gate was off. Dithranol was used as matrix for **1** and **2**, whereas (5,10,15,20-tetrakis(pentafluorophenyl)porphyrin) was used for **3.** The arrows point out the signals originating from molecular ions.

A

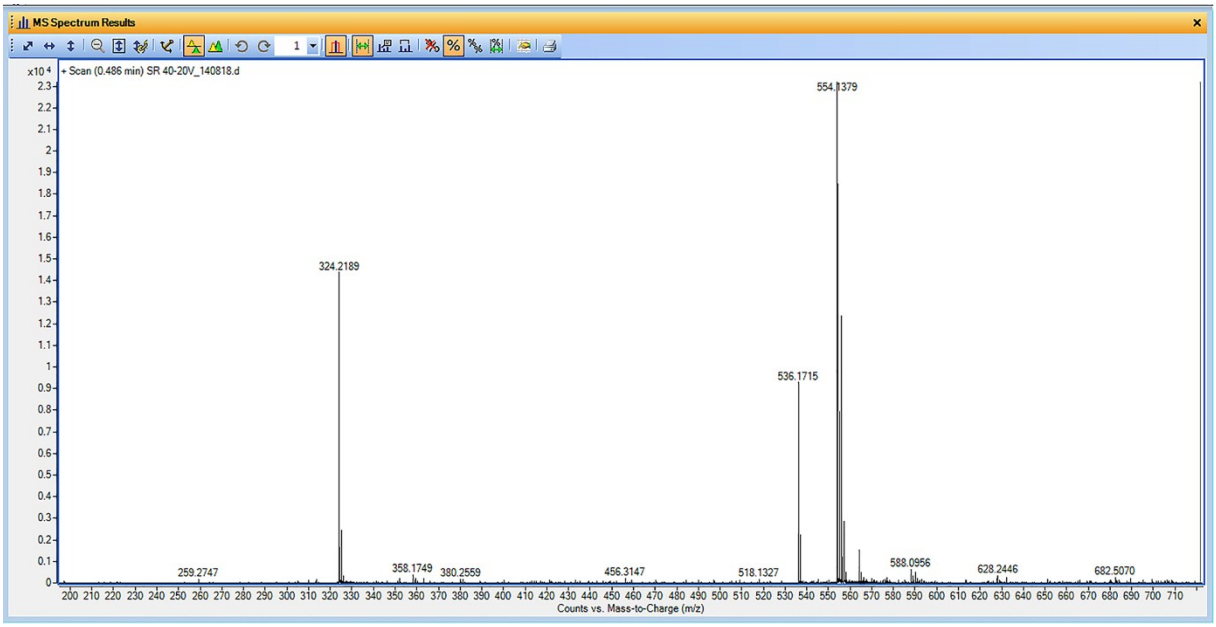
MS Spectrum Results
+ Scan (0.486 min) SR 40-20V_140818.d
554.1379
324.2189
536.1715
259.2747
358.1749
380.2559
456.3147
518.1327
588.0956
628.2446
682.5070
Counts vs. Mass-to-Charge (m/z)

B

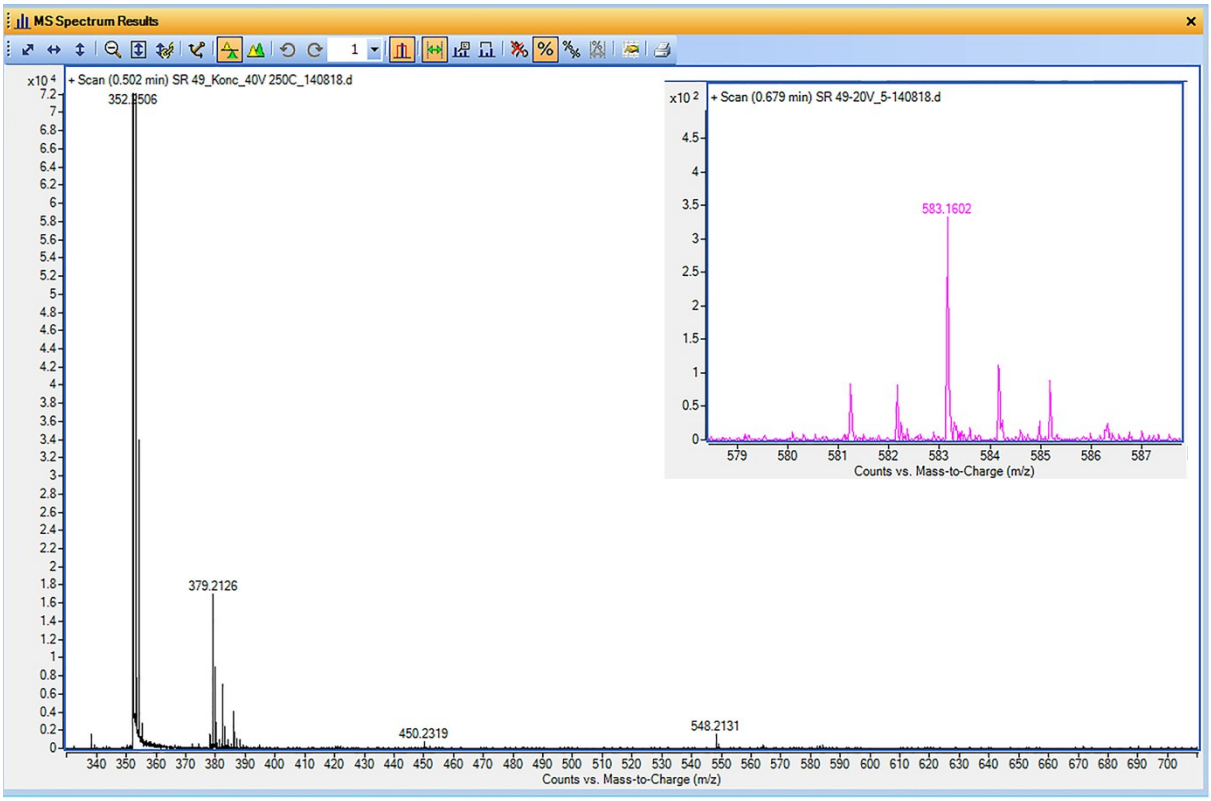
MS Spectrum Results
+ Scan (0.502 min) SR 49_Konc_40V 250C_140818.d
352.2506
379.2126
450.2319
548.2131
+ Scan (0.679 min) SR 49-20V_5-140818.d
583.1602
Counts vs. Mass-to-Charge (m/z)

C

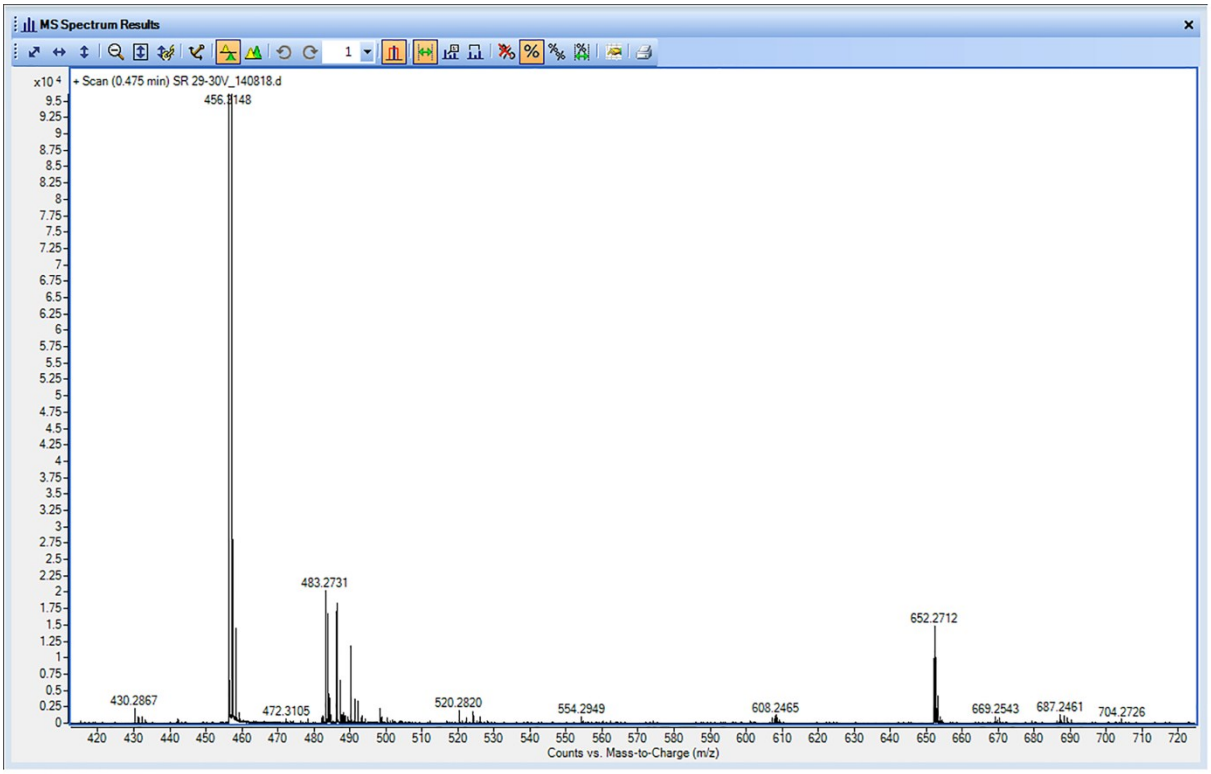

Fig. S6. ESI Q-TOF mass spectra of the complexes **1** (A), **2** (B) and **3** (C) in methanol. The spectra were acquired in the positive ion mode. Instrumental settings were as follows: capillary voltage 3.5 kV, nitrogen desolvation gas flow at 12 L min^{-1}, the source and desolvation temperatures were kept at 250 °C. The skimmer voltage was 20 V, 40 V and 30 V for **1**, **2** and **3**, respectively. The inset in **B** represents a magnification of the signal from the molecular ion of complex **2**, which is not visible in the spectrum B.

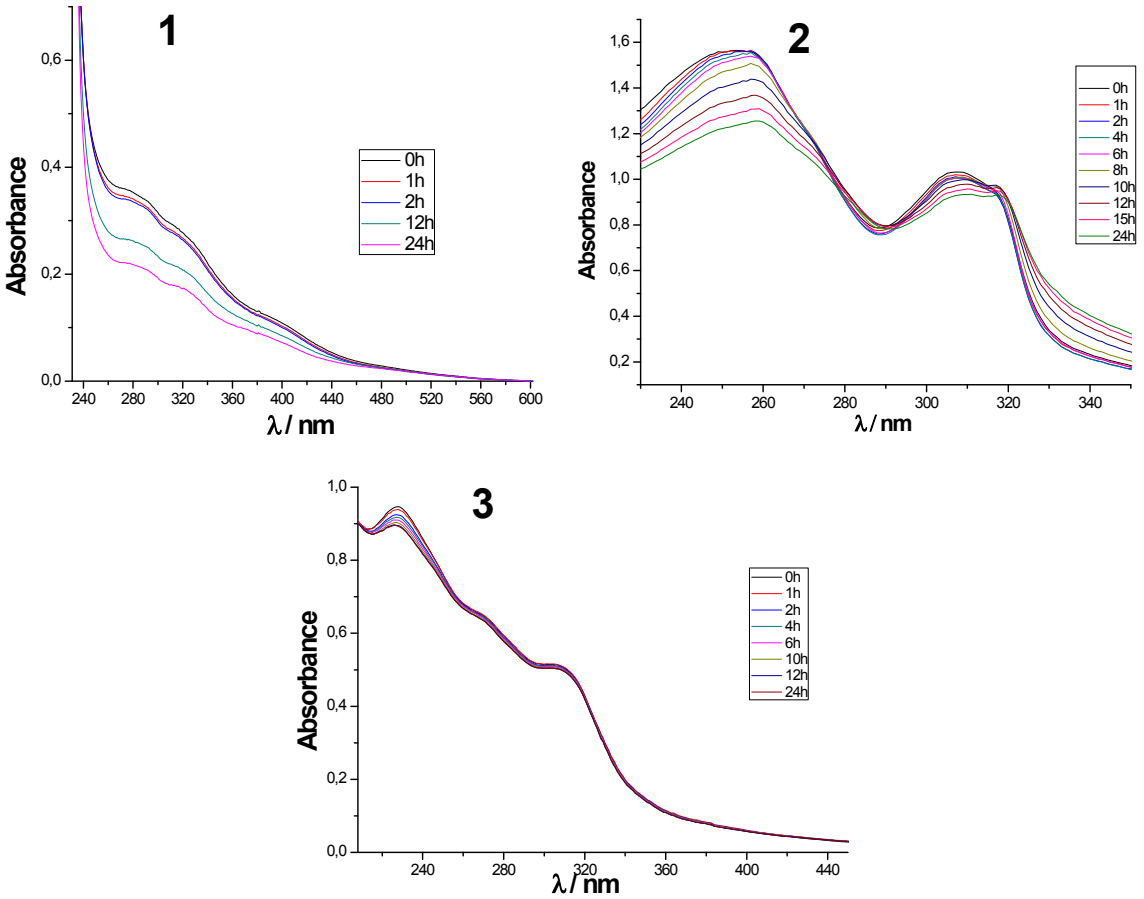

Fig. S7. UV-Vis spectra of complexes **1** – **3** in water over a 24 h period. [Au(III)] = 5 x 10^{-5} M, T = 25 ºC.

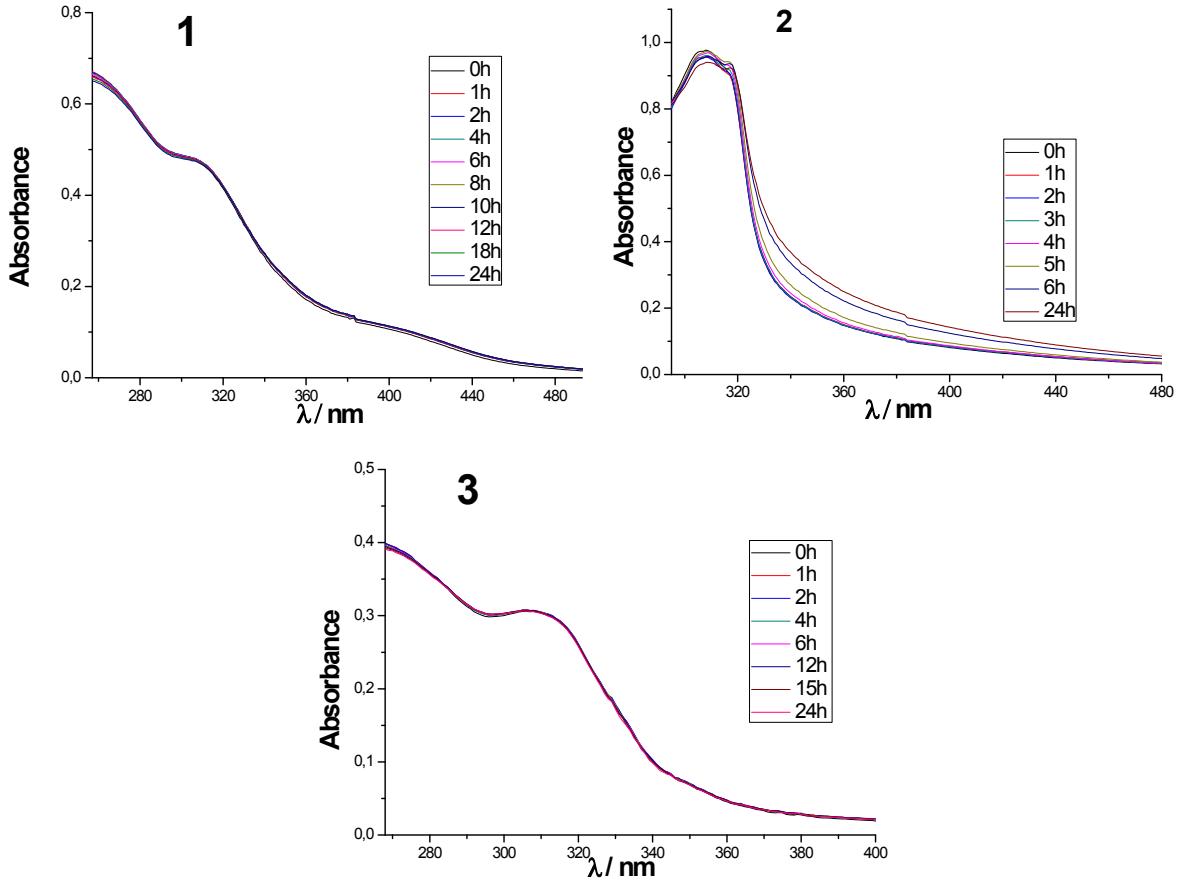

Fig. S8. UV-Vis spectra of complexes **1 – 3** in phosphate buffer (pH = 7.4) over a 24 h period. [Au(III)] = 5 x 10^{-5} M, T = 25 ºC.

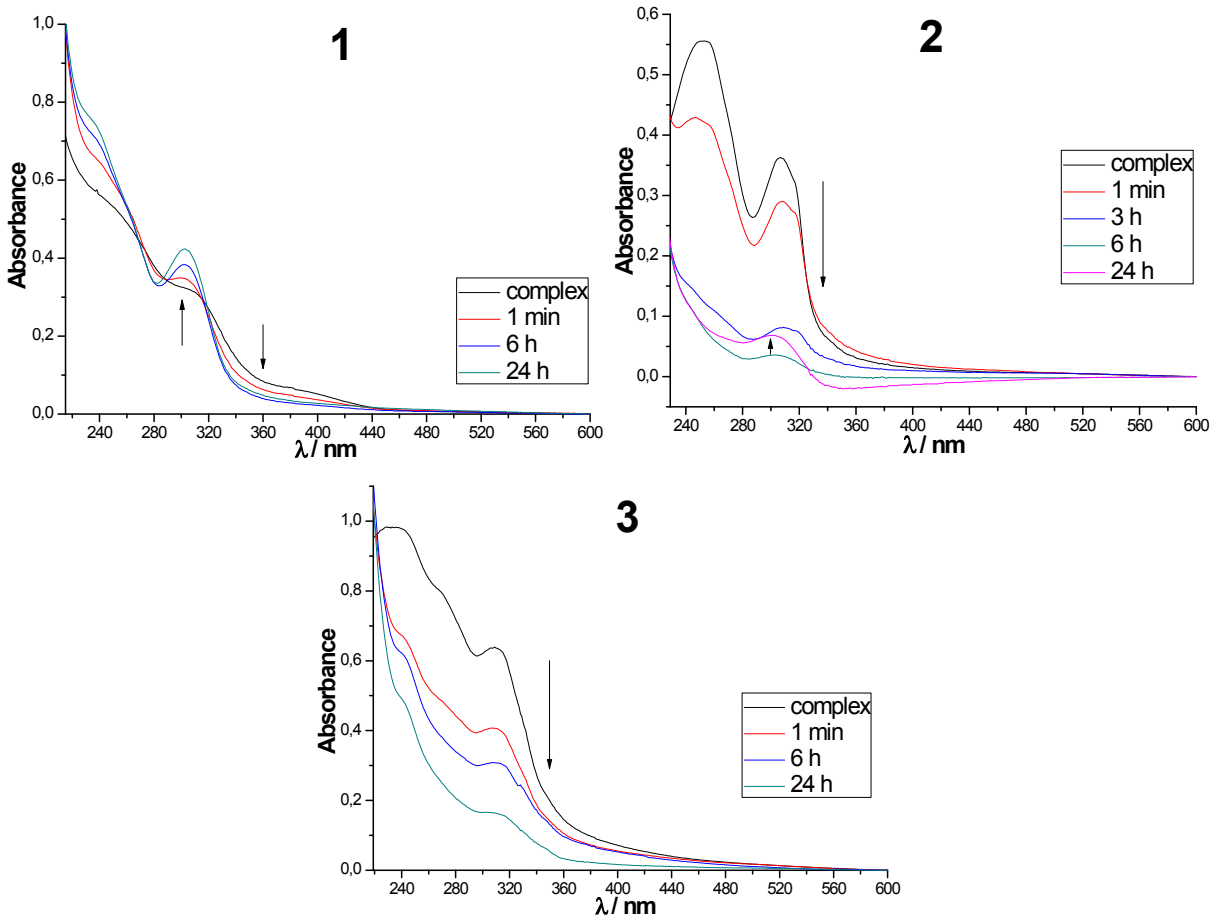

Fig. S9. Time-dependent UV-Vis spectra (up to 24 h) of complexes **1 – 3** dissolved in 10 mM Tris-HCl/150 mM NaCl, pH=7.4 in the presence of GSH 1.5×10^{-4}, [complex]/[GSH] = 1:3 molar ratio. UV-Vis spectra of the complexes without GSH are shown in parallel (black lines).

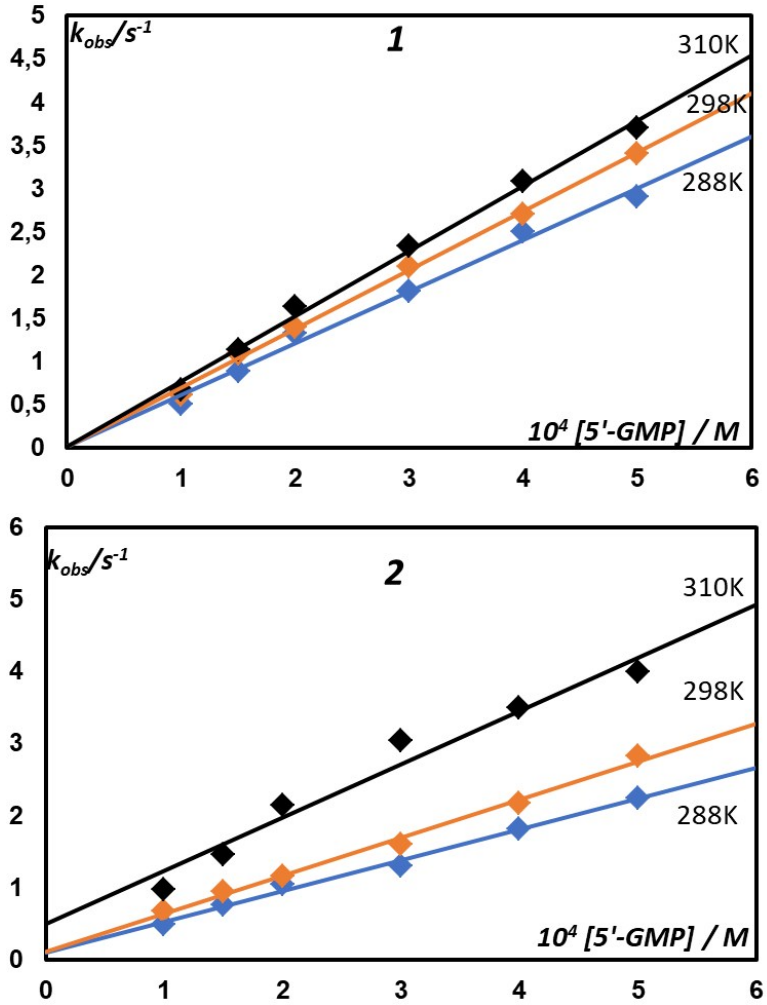

Fig. S10. *Pseudo*-first order rate constants, k_{obs}, as a function of nucleophile concentration and temperature for the substitution reaction of complexes **1** and **2** with 5'-GMP in 10 mM Tris-HCl/150 mM NaCl (pH=7.4).

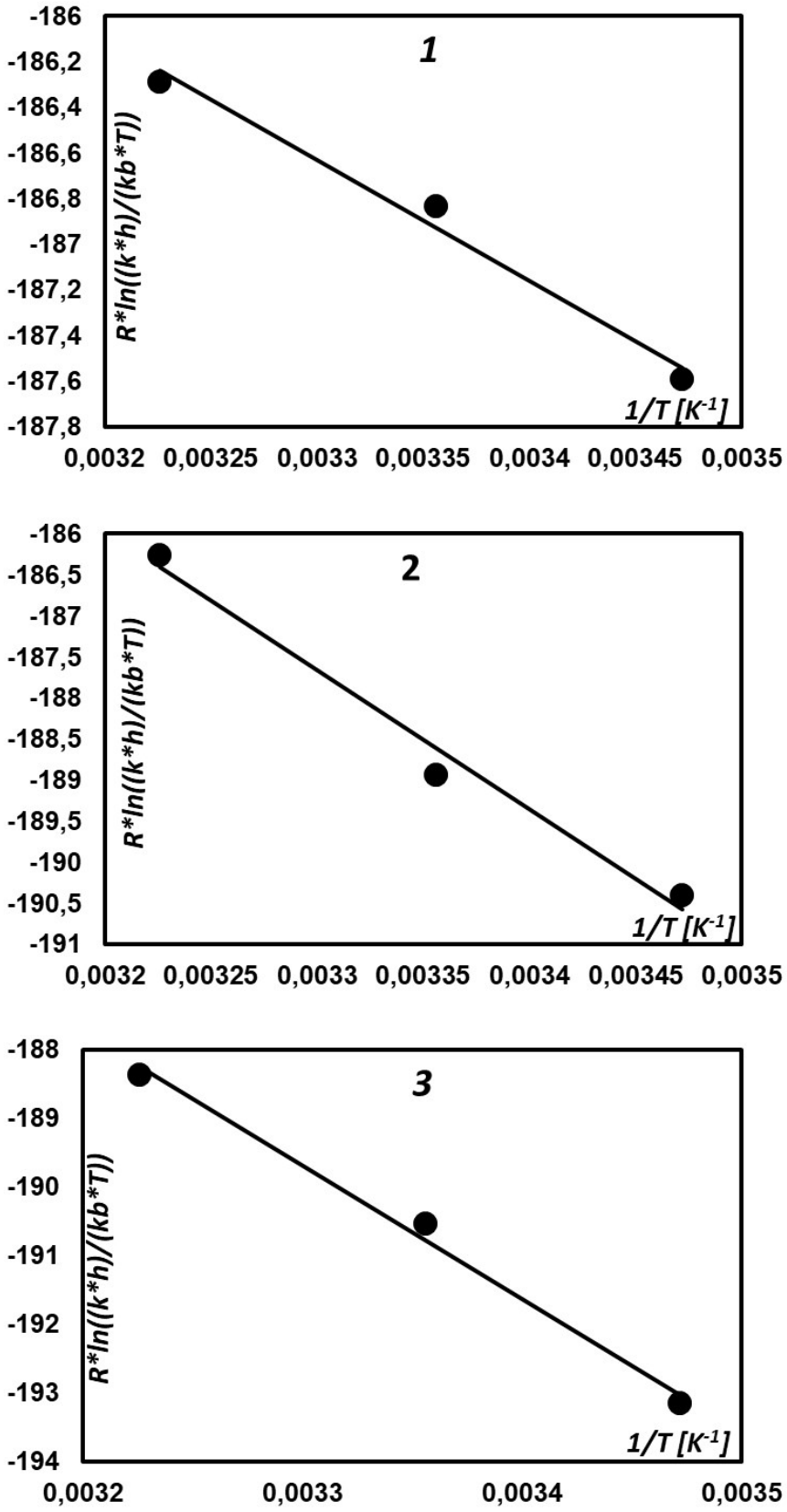

Fig. S11. Eyring plots for the reactions of complexes **1 – 3** with 5'-GMP in 10 mM Tris-HCl/150 mM NaCl (pH=7.4).

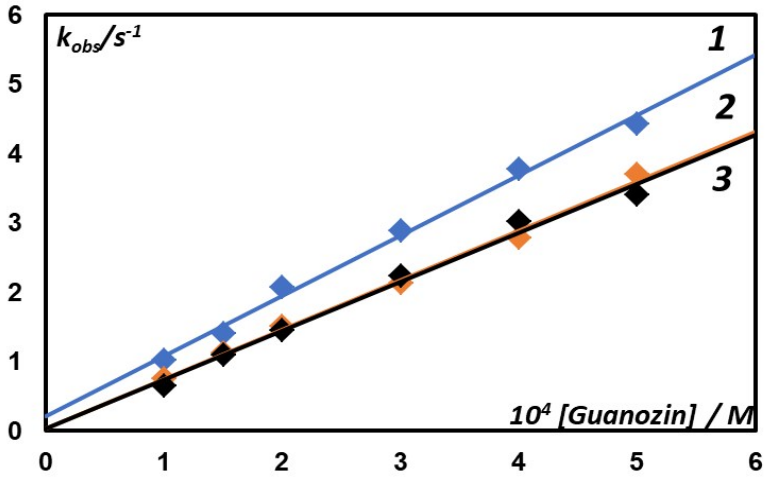

Fig. S12. *Pseudo*-first order rate constants, k_{obs}, as a function of nucleophile concentration for the substitution reactions of complexes **1** – **3** with Guo in 10 mM Tris-HCl/150 mM NaCl (pH=7.4) at 310 K.

DNA-binding studies

Calculation of DNA-binding constants

In order to compare the binding strengths of the complexes, the intrinsic binding constants K_b were determined by monitoring the changes in absorption at the MLCT bands with increasing concentration of CT DNA using the following equation (S1)[S1]

$$[DNA]/(\varepsilon_A - \varepsilon_f) = [DNA]/(\varepsilon_b - \varepsilon_f) + 1/[K_b(\varepsilon_b - \varepsilon_f)] \quad (S1)$$

K_b is given by the ratio of slope to the *y* intercept in plots $[DNA]/(\varepsilon_A - \varepsilon_f)$ *versus* [DNA] (Fig. S13), where [DNA] is the concentration of DNA in base pairs, $\varepsilon_A = A_{obs}/[complex]$, ε_f is the extinction coefficient of the unbound complex and ε_b is the extinction coefficient of the complex in the fully bound form.

Stern-Volmer equation for EB competitive studies

The relative binding of complexes to CT-DNA is described by Stern-Volmer equation (S2)[S2]:

$$I_0/I = 1 + K_{sv}[Q] \quad (S2)$$

where I_0 and I are the emission intensities in the absence and the presence of the quencher (complexes **1, 2** or **3**), respectively, [Q] is the total concentration of quencher, K_{sv} is the Stern-Volmer quenching constant, which can be obtained from the slope of the plot of I_0/I *versus* [Q] (Fig. S15).

References

S1. A. M. Pyle, J. P. Rehmann, R. Meshoyrer, C. V. Kumar, N. J. Turro and J. K. Barton, *J. Am. Chem. Soc*., 1989, **111**: 3051-3058.

S2. R. Lakowicz and G. Weber, *Biochemistry*, 1973, **12**: 4161-4170.

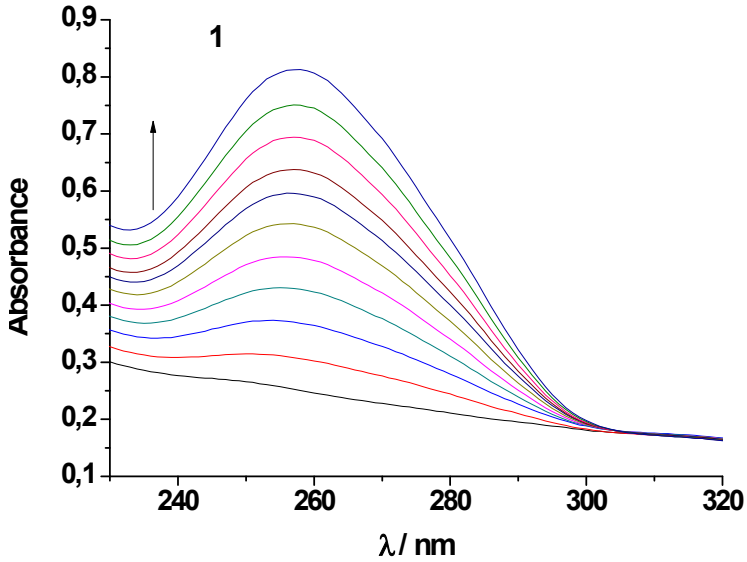
1
Absorbance
0,9
0,8
0,7
0,6
0,5
0,4
0,3
0,2
0,1
240
260
280
300
320
λ / nm

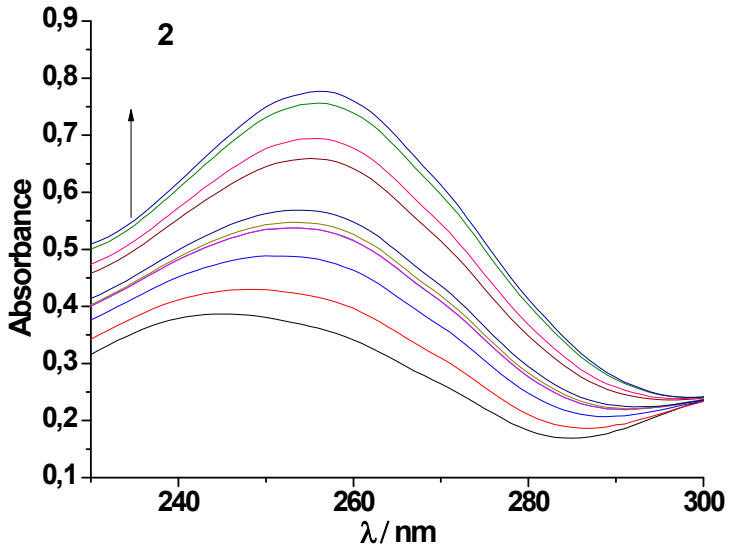
2
Absorbance
0,9
0,8
0,7
0,6
0,5
0,4
0,3
0,2
0,1
240
260
280
300
λ / nm

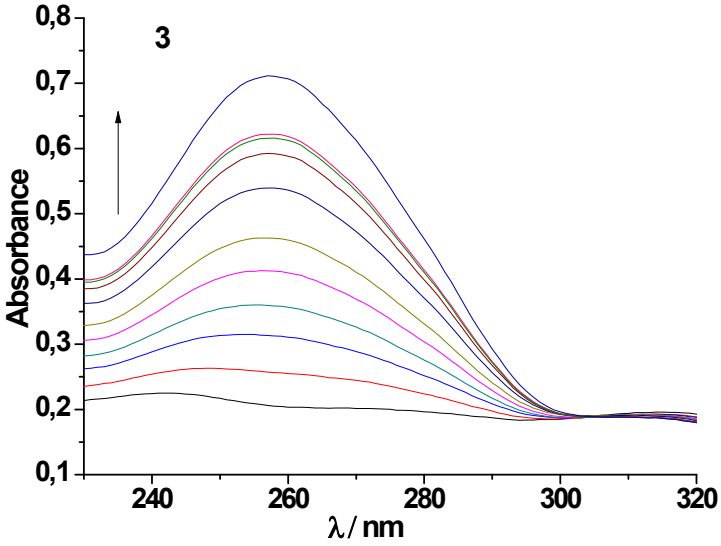
3
Absorbance
0,8
0,7
0,6
0,5
0,4
0,3
0,2
0,1
240
260
280
300
320
λ / nm

Fig. S13. Absorption spectra of the complexes **1 – 3** in 10 mM Tris-HCl/150 mM NaCl pH = 7.4, upon addition of CT DNA. [Au] = 1.35 x 10^{-5} M, [DNA] = (1.35-13.5) x 10^{-5} M. Arrows show the absorbance changes upon addition of increasing amounts of DNA.

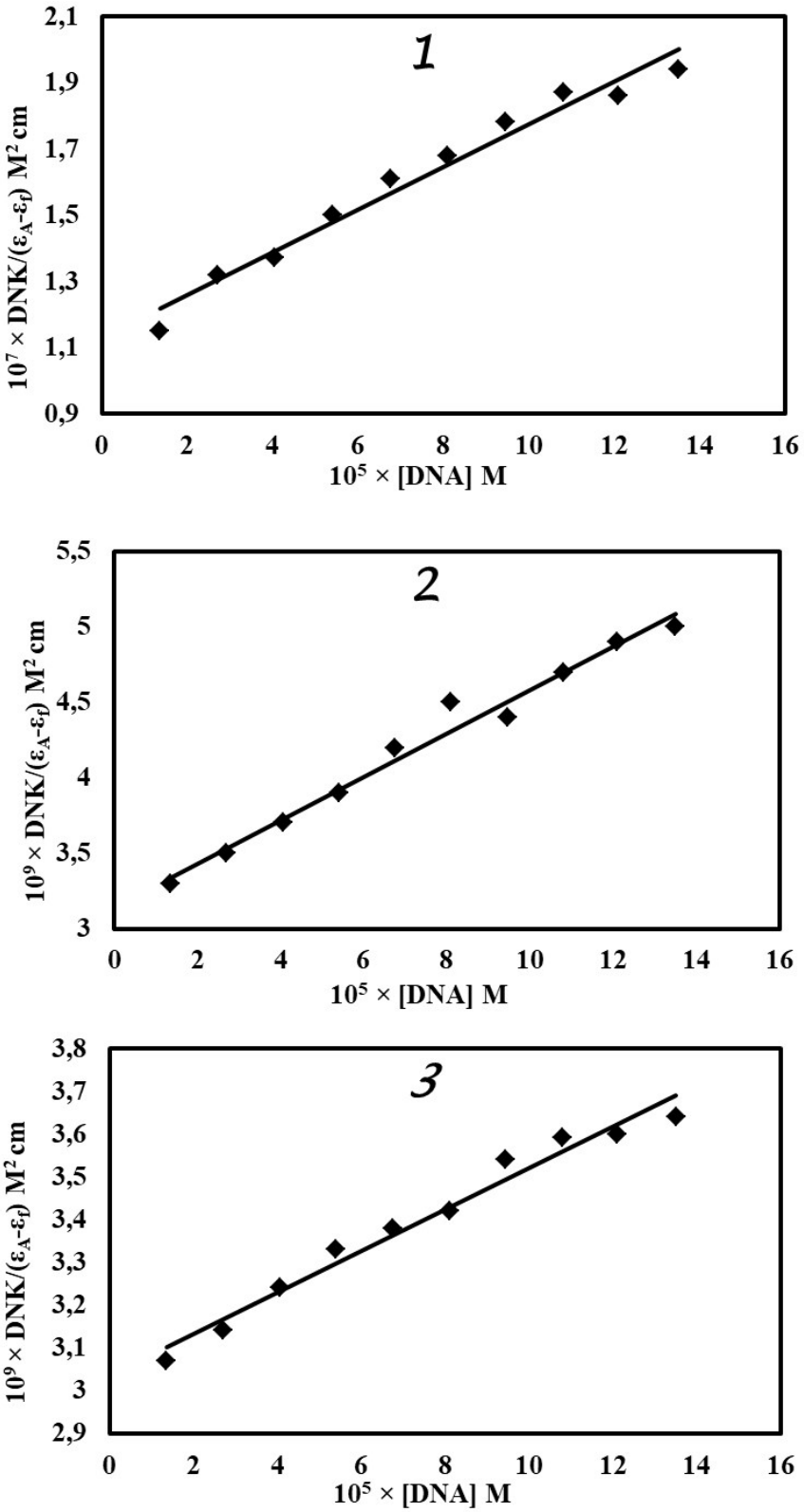

Fig. S14. Plots of [DNA]/($\varepsilon_A - \varepsilon_f$) *versus* [DNA] for complexes **1 – 3**.

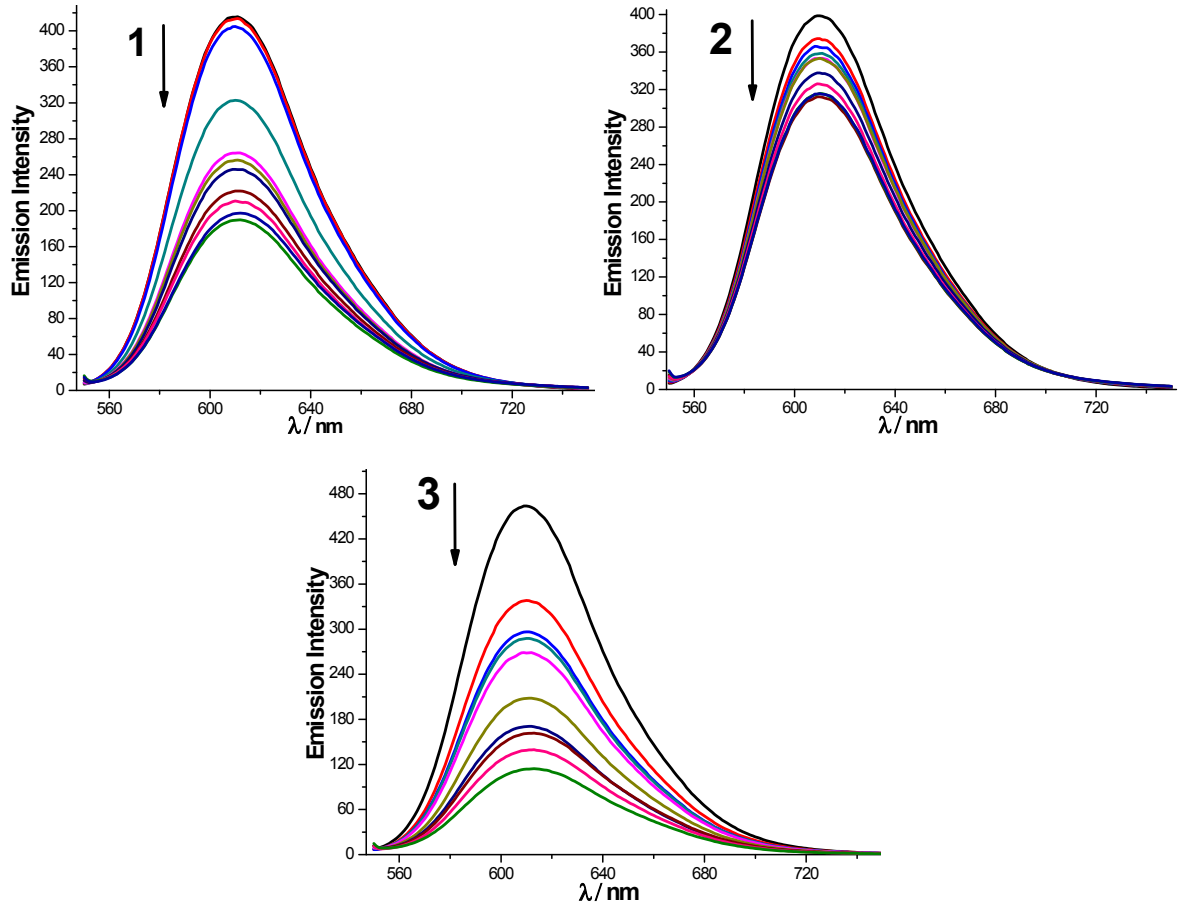

Fig. S15. Emission spectra of EB bound to DNA in the presence of complexes **1** – **3**. [EB] = 80 μM, [DNA] = 80 μM; [Au] = 0–80 μM; λ_{ex} = 527 nm, λ_{em} = 612 nm. The arrows show the intensity changes upon titration with increasing amounts of the complexes **1** – **3**.

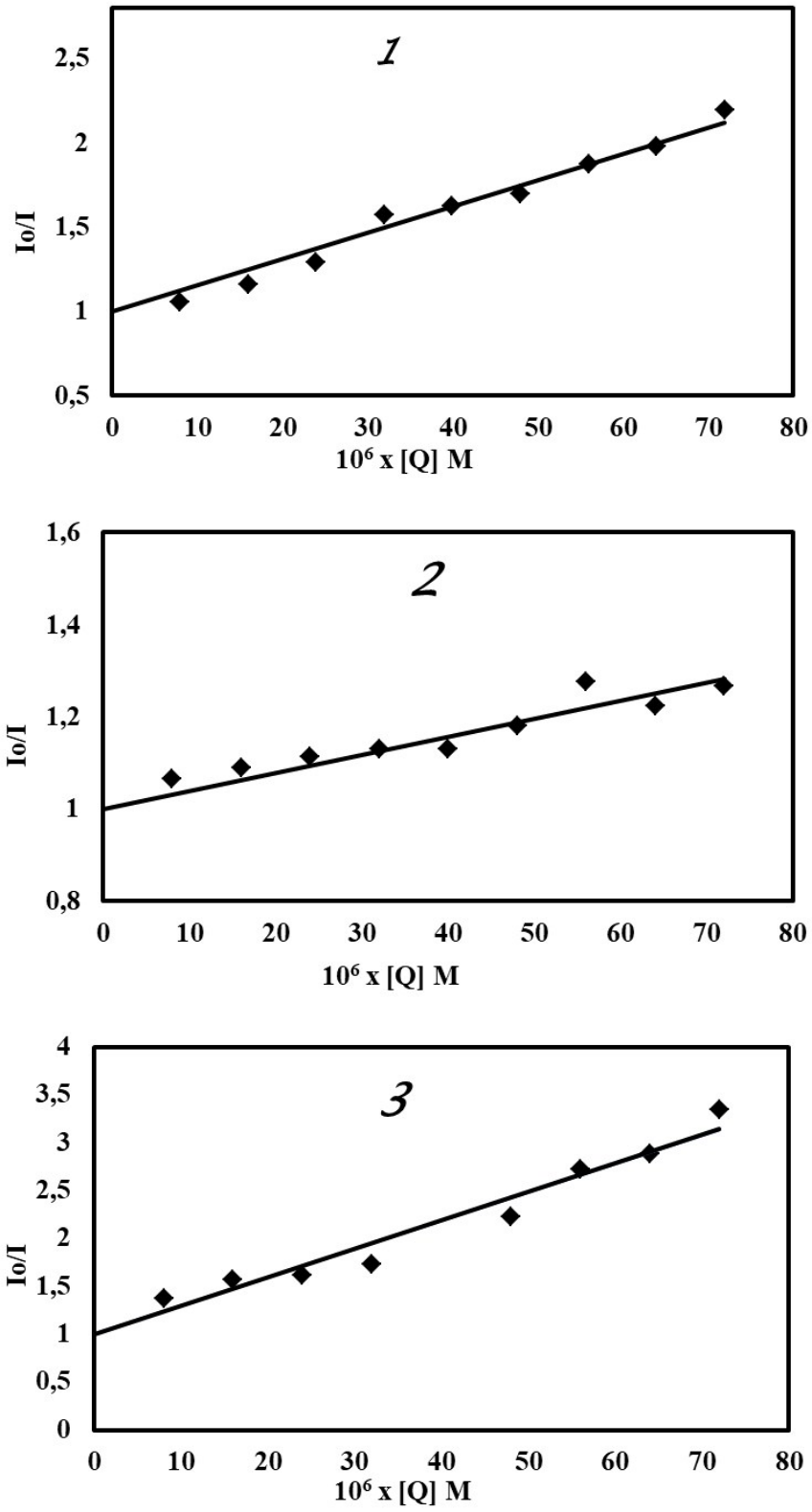

Fig. S16. Stern-Volmer quenching plots of EB-DNA for complexes **1 – 3**.

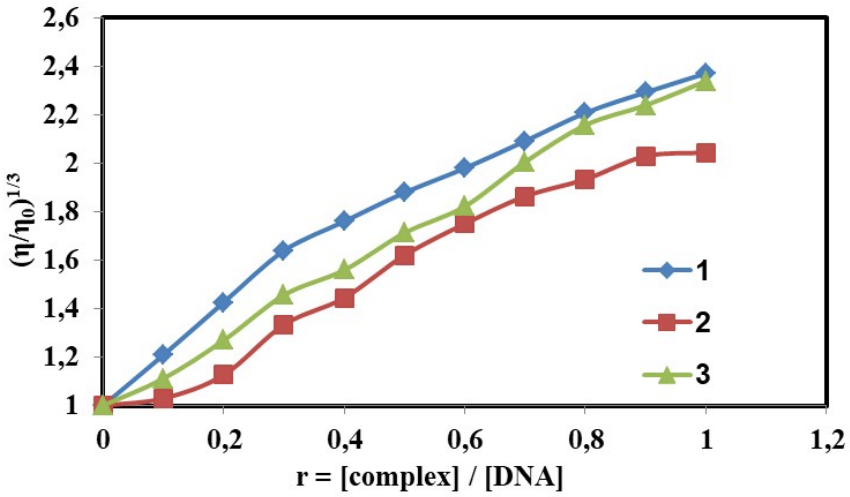

Fig. S17. Relative viscosity $(\eta/\eta_o)^{1/3}$ of CT DNA (0.01mM) in 10 mM Tris-HCl/150 mM NaCl, pH=7.4) in the absence/presence of the increasing amounts of complexes **1** – **3** (r).

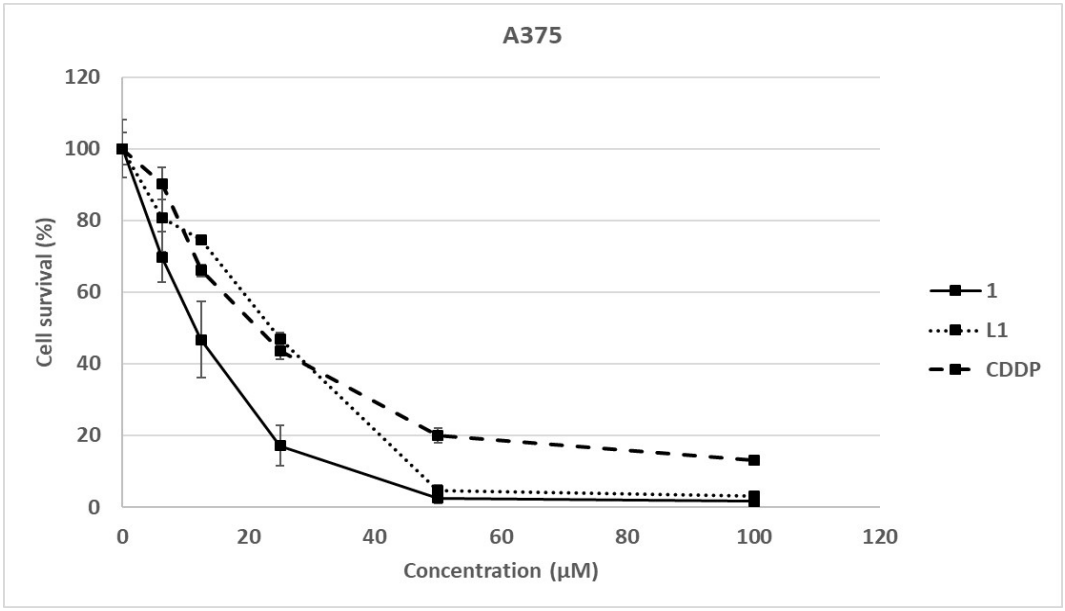
A375
Cell survival (%)
120
100
80
60
40
20
0
0
20
40
60
80
100
120
Concentration (μM)
1
L1
CDDP

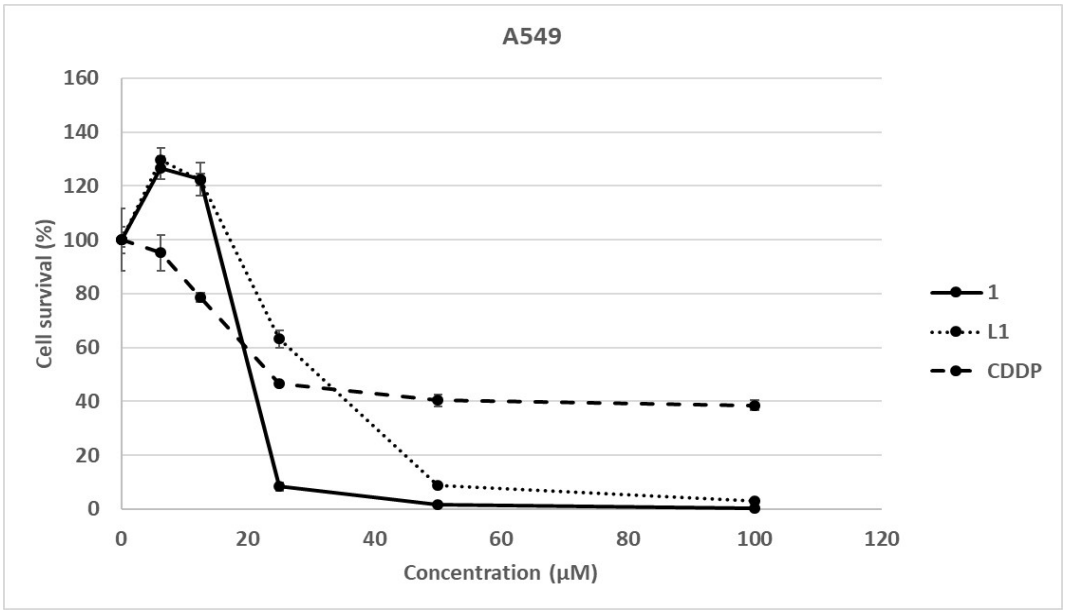
A549
Cell survival (%)
160
140
120
100
80
60
40
20
0
0
20
40
60
80
100
120
Concentration (μM)
1
L1
CDDP

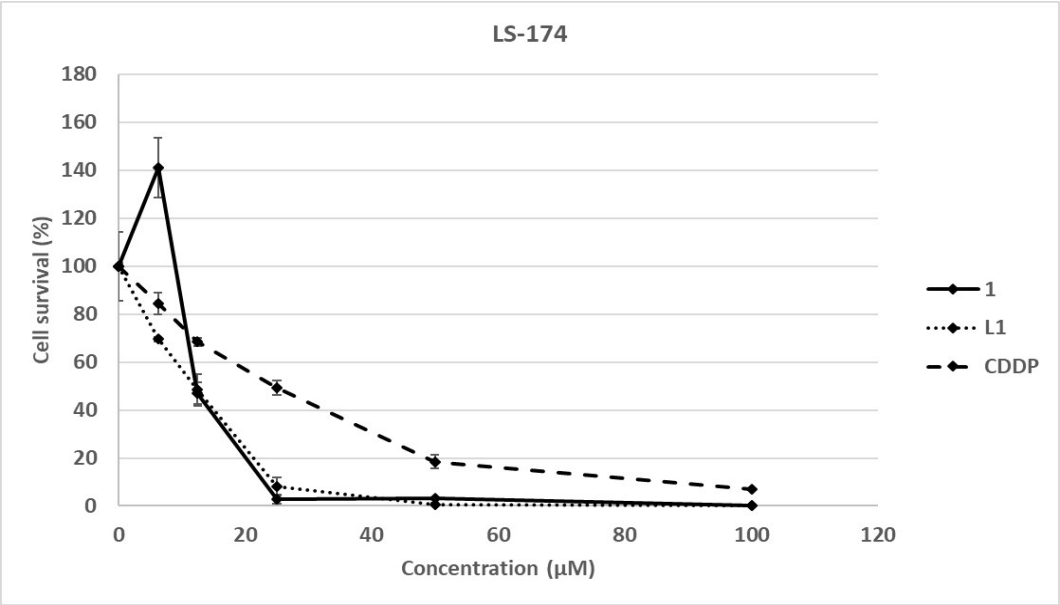

Fig. S18. Cell survival diagrams of A375, A549 and LS-174 after 48 h of their continual exposure to the investigated compounds (**1** = complex **1**, L1 = H_2L^{tBu} - ligand of complex **1** and CDDP =cisplatin). Data are representative for one out of three separate experiments with standard deviations.

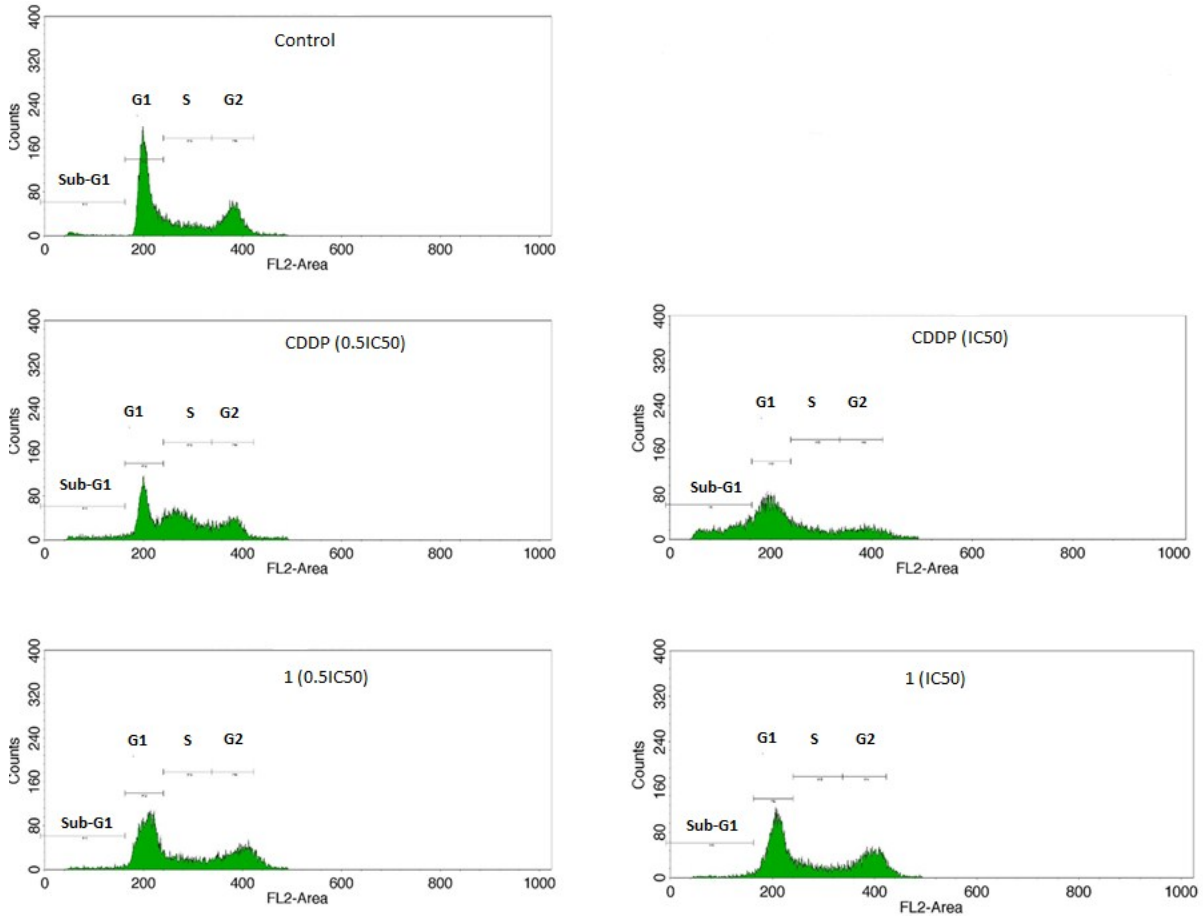

	Control	1 (0.5IC50)	1 (IC50)	CDDP (0.5IC50)	CDDP (IC50)
Sub-G1	1.56	3.33	3.11	5.53	21.91
G1	51.35	45.88	44.09	32.83	42.21
S	19.46	19.04	19.69	37.93	18.11
G2	26.42	25.67	29	21.95	14.4

Fig. S19. Effects of the gold complex (**1**) and cisplatin (CDDP) on cell cycle progression of A375 cells, following 24 h incubation with concentrations corresponding to 0.5IC50 and IC50. Controls were untreated cells (incubated with nutrient medium only). Shown histograms are representative of three independent experiments. Table summarizes percentage of cells in different cell cycle phases, which are drawn from the presented histograms.

Table S1. Assignments of ^{1}H resonances (δ) for the ligands $\mathbf{H_2L^{tBu}}$, $\mathbf{Me_2L^{tBu}}$, $\mathbf{Me_2{}^*L}$ and complexes **1** – **3** in CD_3OD.

	$\mathbf{H_2L^{tBu}}$	**1**	$\mathbf{Me_2L^{tBu}}$	**2**	$\mathbf{Me_2{}^*L}$	**3**
C3*H*/C5*H*	7.71	7.66	7.79	7.88	7.70	7.86
C4*H*	7.84	8.15	7.81	8.00	7.75	8.22
C8H/C8'H	6.79	6.86	6.84	6.88		
N10C*H*$_3$/N10'C*H*$_3$			4.07	4.09	3.90	4.03
C12(C*H*$_3$)$_3$/C12'(C*H*$_3$)$_3$	1.40	1.36	1.49	1.47		
C12*H*/C12'*H*					3.32 – 3.28	3.33 – 3.27
C13*H*$_2$/C13'*H*$_2$					2.21 – 2.13 & 1.37 – 1.25	2.28 – 2.20 & 1.27 – 1.20
C14*H*$_2$/C14'*H*$_2$					1.98 – 1.91 & 1.37 – 1.25	2.03 – 1.96 & 1.40 – 1.33
C15C*H*$_3$/C15'C*H*$_3$					1.44	1.47
C16(C*H*$_3$)$_2$/C16'(C*H*$_3$)$_2$					0.99 & 0.82	1.04 & 0.85

Table S2. The peaks detected in the MALDI TOF mass spectra of the complexes **1**-**3**.

Peak position (*m/z*)	*m/z* range	Peak assignment
complex 1		
311.81	309.85-313.70	$[M\text{-}AuCl\text{-}(CH_3)+4H^+]^+$
327.65	327.67-330.68	$[M\text{-}AuCl+4H^+]^+$
345.71	345.71-347.66	n.a.
361.46	361.45-363.43	n.a.
518.81	518.81-520.78	$[M\text{-}Cl\text{-}2H]^+$
540.57	540.57-542.52	$[M\text{-}(CH_3)]^+$
556.27	556.27-560.32	$[MH]^+$
590.05	590.05-592.06	$\{[M]Cl\}^+$
623.88	623.89-627.73	n.a.
complex 2		
476.53	474.54-479.54	$\{[M\text{-}2CH_3\text{-}2tBu+3H]Cl\}^+$
547.54	545.57-548.54	$[M\text{-}Cl\text{-}H]^+$
582.38	579.44-584.39	$[M\text{-}H^+]^+$
621.23	621.23-623.23	$\{[M+3H]Cl\}^+$
complex 3		
412.16	406.15-416.09	n.a.
456.48	450.35-459.22	$[M\text{-}AuCl+H]^+$
490.26	480.29-493.24	$\{[M\text{-}AuCl]Cl\}^+$
520.25	514.25-526.23	$\{[M\text{-}AuCl+2CH_3]Cl\}^+$
554.21	550.19-558.21	$\{[M\text{-}Au+2CH_3\text{-}H]Cl\}^+$
650.21	648.22-654.31	$[M\text{-}Cl\text{-}2H^+]^+$
688.14	687.14-689.14	$[MH]^+$

Table S3. The signals detected in the ESI Q-TOF mass spectra of the complexes **1**-**3**.

Signal position (*m/z*)	calculated *m/z*	Peak assignment
complex 1		
324.2189	324.2188	$[M\text{-}AuCl+H]^+$
536.1715		n.a.
554.1379	554.1386	$[M\text{-}H]^+$
complex 2		
352.2506	352.2501	$[M\text{-}AuCl+H]^+$
379.2126		n.a.
450.2319		n.a.
548.2131	548.2089	$[M\text{-}Cl]^+$
583.1602	583.1777	$[M]^+$
complex 3		
456.3148	456.3127	$[M\text{-}AuCl+H]^+$
483.2731		n.a.
652.2712	652.2715	$[M\text{-}Cl]^+$
687.2461	687.2403	$[M]^+$

Table S4. Observed *pseudo*-first order rate constants as a function of complex concentration for the reaction between complexes **1**, **2** or **3** and 5'-GMP (**L**)

288K

Complex	C_L [10^{-4} M]	k_{obs} [s^{-1}]
$H_2L^{t\text{-}Bu}$ **(1)**	5.0	2.90
	4.0	2.50
	3.0	1.81
	2.0	1.32
	1.5	0.89
	1.0	0.51
$Me_2L^{t\text{-}Bu}$ **(2)**	5.0	2.25
	4.0	1.82
	3.0	1.31
	2.0	1.05
	1.5	0.76
	1.0	0.49
Me_2^*L **(3)**	5.0	1.60
	4.0	1.35
	3.0	1.07
	2.0	0.79
	1.5	0.54
	1.0	0.37

298K

Complex	C_L [10^{-4} M]	k_{obs} [s^{-1}]
$H_2L^{t\text{-}Bu}$ **(1)**	5.0	3.37
	4.0	2.74
	3.0	2.14
	2.0	1.40
	1.5	1.09
	1.0	0.61
$Me_2L^{t\text{-}Bu}$ **(2)**	5.0	2.83
	4.0	2.18
	3.0	1.61
	2.0	1.16
	1.5	0.95
	1.0	0.68
Me_2^*L **(3)**	5.0	2.25
	4.0	1.84
	3.0	1.50
	2.0	1.05
	1.5	0.79
	1.0	0.46

310K

Complex	C_L [10^{-4} M]	k_{obs} [s^{-1}]
$H_2L^{t\text{-}Bu}$ **(1)**	5.0	3.7
	4.0	3.08
	3.0	2.33
	2.0	1.63
	1.5	1.13
	1.0	0.67
$Me_2L^{t\text{-}Bu}$ **(2)**	5.0	4.00
	4.0	3.50
	3.0	3.04
	2.0	2.15
	1.5	1.46
	1.0	0.98
$Me_2{}^*L$ **(3)**	5.0	3.11
	4.0	2.53
	3.0	1.94
	2.0	1.46
	1.5	1.06
	1.0	0.72

Table S5. Observed *pseudo*-first order rate constants as a function of complex concentration for the reaction between complexes **1**, **2** or **3** and guanosine (**L**)

Complex	C_L [10^{-4} M]	k_{obs} [s^{-1}]
$H_2L^{t\text{-}Bu}$ **(1)**	5.0	4.43
	4.0	3.78
	3.0	2.89
	2.0	2.07
	1.5	1.41
	1.0	1.02
$Me_2L^{t\text{-}Bu}$ **(2)**	5.0	3.70
	4.0	2.78
	3.0	2.13
	2.0	1.51
	1.5	1.13
	1.0	0.75
Me_2^*L **(3)**	5.0	3.40
	4.0	3.02
	3.0	2.24
	2.0	1.45
	1.5	1.09
	1.0	0.65

Table S6. Observed *pseudo*-first order rate constants, k_{obs}, as a function of complex concentration for the reaction between complexes **1**, **2** or **3** and CT DNA (**L**)

Complex	C_L [10^{-4} M]	k_{obs} [s^{-1}]
$H_2L^{t\text{-}Bu}$ **(1)**	5.0	5.01
	4.0	3.94
	3.0	3.09
	2.0	2.28
	1.5	1.62
	1.0	1.10
$Me_2L^{t\text{-}Bu}$ **(2)**	5.0	3.92
	4.0	3.05
	3.0	2.47
	2.0	1.69
	1.5	1.26
	1.0	0.77
Me_2^*L **(3)**	5.0	3.55
	4.0	3.15
	3.0	2.35
	2.0	1.57
	1.5	1.18
	1.0	0.72